Materials Physics and Mechanics 37 (2018) 16-24 Received: December 22, 2017

# MODELS OF POROUS PIEZOCOMPOSITES WITH 3-3 CONNECTIVITY TYPE IN ACELAN FINITE ELEMENT PACKAGE

**A.B. Kudimova[1], D.K. Nadolin[1], A.V. Nasedkin[1], A.A. Nasedkina[1], P.A. Oganesyan[1], A.N. Soloviev[1,2*]**

[1]I.I. Vorovich Institute of Mathematics, Mechanics and Computer Sciences,
Southern Federal University, Miltchakova str., 8a, Rostov-on-Don, 344090, Russia

[2]Department of Theoretical and Applied Mechanics, Don State Technical University,
Gagarin Sq., 1, Rostov-on-Don, 344000, Russia

*e-mail: solovievarc@gmail.com

**Abstract.** The work deals with the methods for solving homogenization problems for porous piezoceramic media with open porosity, which are implemented in ACELAN-COMPOS finite element software package developed by the authors. Determination of the effective properties of composite media is based on the effective moduli method and the finite element method. Special algorithm was developed to generate representative volumes for two-phase composites that support connectivity for both phases. The work of the suggested algorithm is illustrated by an example of porous piezoceramic PZT-4. Numerical experiments show that the representative volume structure can have a significant effect on the effective moduli of a piezoceramic with open porosity.

**Keywords:** piezoelectricity; 3-3 two-phase piezocomposite; effective moduli; representative volume; finite element method; finite element software.

## 1. Introduction

In the recent time, an increased interest has been observed to the investigations of composite materials of complex structure that exhibit very effective properties for many practical applications. Thus, porous piezoceramic materials have received considerable attention due to their application in ultrasonic transducers, hydrophones, pressure sensors and other piezoelectric devices. The classification of piezoelectric composites was initiated by Newnham's connectivity theory. According to this theory, a porous piezoceramic can be classified as a two-phase composite. As is well known, the 3-0 (with closed porosity) and 3-3 (with open porosity) piezocomposites in the form of porous piezoelectric materials show considerably improved transducer characteristics. Porous piezocomposites have great potential for low acoustic impedance and higher efficiency compared to conventional dense piezoceramic materials [1, 2].

For computer simulation of porous piezocomposites, we have developed new ACELAN-COMPOS module, which is a part of our own developed finite element software – ACELAN package. ACELAN was developed about 15 years ago and was initially intended for computer simulation of piezoelectric devices. Later releases of ACELAN package contained not only the models of elastic, piezoelectric and acoustic media, but were also capable to solve more complicated coupled problems with connectivity of mechanical, electrical and magnetic fields. The ACELAN-COMPOS module has been specially developed

http://dx.doi.org/10.18720/MPM.3712018_3

to solve the problem of the active composite homogenization by using the effective moduli method and finite element technologies. Original algorithms for generating representative volumes of 3-0 and 3-3 porous composites have been developed and implemented in ACELAN-COMPOS. Thus, the structure of 3-0 porous composites is modeled by using an algorithm that generates a representative volume with granular inclusions. At the same time, 3-3 porous composites are simulated by using an algorithm that forms connected structures for each component of the two-phase composite media.

This paper focuses on the algorithm for simulating composite materials with 3-3 connectivity. We model these materials using cubic elements (octants) in the representative volume. Initial volume is divided into octants, using Octree algorithm, where the size and the number of elements may vary depending on the physical properties of the material or the required accuracy. Octants can be then easily used as finite elements on a regular mesh. Structural elements of the same materials are united into the composite components. Each component has a communication property: any element, belonging to the component, is reachable from any other component element by a transition between adjacent elements. This approach allows us to model 3-3 porous composites and materials with mixtures. The results of numerical experiments in ACELAN-COMPOS show that the structures of the representative volumes can significantly affect the values of the effective moduli for porous piezocomposites, especially when one of the phases has large inclusion parts.

## 2. Homogenization of porous piezoceramic material by the effective moduli method

Let $\Omega$ is a representative volume of a porous piezoceramic material; $\Omega = \Omega^{(1)} \cup \Omega^{(2)}$, $\Omega^{(1)}$ is the skeleton of piezoceramic material; $\Omega^{(2)}$ is the second connected volume of open porosity; $\Gamma = \partial\Omega$ is the external boundary of the volume $\Omega$; $\mathbf{x} = \{x_1, x_2, x_3\}$ is the vector of spatial coordinates.

In accordance with general theory of effective moduli for piezoelectric composites [3, 4], we consider the following static piezoelectric boundary problem ($i = 1, 2, 3$; $\alpha = 1, 2, ..., 6$):

$$\sigma_{ij,j} = 0,\ D_{j,j} = 0,\ T_\alpha = c_{\alpha\beta} S_\beta - e_{j\alpha} E_j,\ D_i = e_{i\beta} S_\beta + \kappa_{ij} E_j, \tag{1}$$

$$\varepsilon_{ij} = (u_{i,j} + u_{j,i})/2,\ E_i = -\varphi_{,i}, \tag{2}$$

$$u_i = x_j \varepsilon_{0ij},\ \varphi = -x_j E_{0j},\ \mathbf{x} \in \Gamma, \tag{3}$$

where the summation index $j$ runs through the set $\{1, 2, 3\}$, the index $\beta$ runs through the set $\{1, 2, ..., 6\}$; $\sigma_{ij}$ are the components of the stress tensor; $T_k = \sigma_{kk}$, $k = 1, 2, 3$; $T_4 = \sigma_{23}$; $T_5 = \sigma_{13}$; $T_6 = \sigma_{12}$; $S_k = \varepsilon_{kk}$, $k = 1, 2, 3$; $S_4 = 2\varepsilon_{23}$; $S_5 = 2\varepsilon_{13}$; $S_6 = 2\varepsilon_{12}$; $\varepsilon_{ij}$ are the components of the strain tensor; $D_i$ are the components of the electric flux density vector; $E_i$ are the components of the electric field vector; $u_i$ are the components of the vector-function of mechanical displacement; $\varphi$ is the function of electric potential; $c_{\alpha\beta} = c^E_{\alpha\beta}$ are the components of the $6 \times 6$ matrix $\mathbf{c} = \mathbf{c}^E$ of elastic stiffness moduli; $e_{j\alpha}$ are the components of the $3 \times 6$ matrix $\mathbf{e}$ of piezoelectric moduli; $\kappa_{ij} = \varepsilon^S_{ij}$ are the components of the $3 \times 3$ matrix $\boldsymbol{\kappa} = \boldsymbol{\varepsilon}^S$ of dielectric permittivity moduli; $\mathbf{c} = \mathbf{c}^{(i)}$, $\mathbf{e} = \mathbf{e}^{(i)}$, $\boldsymbol{\kappa} = \boldsymbol{\kappa}^{(i)}$ for $\mathbf{x} \in \Omega^{(i)}$; $\varepsilon_{0ij}$ and $E_{0j}$ are some constant values that do not depend on $\mathbf{x}$.

By using (3), we can select such boundary conditions that enable us to obtain obvious expressions for the effective moduli.

Appropriate set of the solutions of these problems allows us to determine the full set of

the effective moduli for the porous piezocomposite. Thus, a piezoceramic, polarized in the direction of $x_3$-axis, is an anisotropic material of a 6*mm* crystallographic class and has 10 independent material moduli (5 elastic moduli, 3 piezoelectric moduli and 2 dielectric moduli):

$$\mathbf{c}=\begin{bmatrix} c_{11} & c_{12} & c_{13} & 0 & 0 & 0 \\ c_{12} & c_{11} & c_{13} & 0 & 0 & 0 \\ c_{13} & c_{13} & c_{33} & 0 & 0 & 0 \\ 0 & 0 & 0 & c_{44} & 0 & 0 \\ 0 & 0 & 0 & 0 & c_{44} & 0 \\ 0 & 0 & 0 & 0 & 0 & c_{66} \end{bmatrix}; \quad \mathbf{e}^{*}=\begin{bmatrix} 0 & 0 & e_{31} \\ 0 & 0 & e_{31} \\ 0 & 0 & e_{33} \\ 0 & e_{15} & 0 \\ e_{15} & 0 & 0 \\ 0 & 0 & 0 \end{bmatrix}; \quad \boldsymbol{\kappa}=\begin{bmatrix} \kappa_{11} & 0 & 0 \\ 0 & \kappa_{11} & 0 \\ 0 & 0 & \kappa_{33} \end{bmatrix},$$

where $c_{66}=(c_{11}-c_{12})/2$.

For this case, the full set of the effective moduli $c_{11}^{\text{eff}}$, $c_{12}^{\text{eff}}$, $c_{13}^{\text{eff}}$, $c_{33}^{\text{eff}}$, $c_{44}^{\text{eff}}$, $e_{31}^{\text{eff}}$, $e_{33}^{\text{eff}}$, $e_{15}^{\text{eff}}$, $\kappa_{11}^{\text{eff}}$, $\kappa_{33}^{\text{eff}}$ can be obtained from the solutions of five problems (1) – (3) with various types of boundary conditions in (3):

I. $\varepsilon_{0ij}=s_0\delta_{i1}\delta_{j1},\ E_{0j}=0 \Rightarrow c_{1k}^{\text{eff}}=\langle\sigma_{kk}\rangle/s_0;\ k=1,2,3;\ e_{31}^{\text{eff}}=\langle D_3\rangle/s_0,$ (4)

II. $\varepsilon_{0ij}=s_0\delta_{i3}\delta_{j3},\ E_{0j}=0 \Rightarrow c_{k3}^{\text{eff}}=\langle\sigma_{kk}\rangle/s_0;\ k=1,2,3;\ e_{33}^{\text{eff}}=\langle D_3\rangle/s_0,$ (5)

III. $\varepsilon_{0ij}=s_0(\delta_{i2}\delta_{j3}+\delta_{i3}\delta_{j2})/2,\ E_{0j}=0 \Rightarrow c_{44}^{\text{eff}}=\langle\sigma_{23}\rangle/s_0;\ e_{15}^{\text{eff}}=\langle D_2\rangle/s_0,$ (6)

IV. $\varepsilon_{0ij}=0,\ E_{0j}=E_0\delta_{1j} \Rightarrow e_{15}^{\text{eff}}=-\langle\sigma_{13}\rangle/E_0;\ \kappa_{11}^{\text{eff}}=\langle D_1\rangle/E_0,$ (7)

V. $\varepsilon_{0ij}=0,\ E_{0j}=E_0\delta_{3j} \Rightarrow e_{3k}^{\text{eff}}=-\langle\sigma_{kk}\rangle/E_0;\ k=1,2,3;\ \kappa_{33}^{\text{eff}}=\langle D_3\rangle/E_0,$ (8)

where $\delta_{ij}$ is the Kronecker symbol; hereinafter the angle brackets denote the averaged by the volume $\Omega$ values: $<(...)>=(1/|\Omega|)\int_{\Omega}(...)d\Omega$.

In this approach we assume that the phase $\Omega^{(2)}$, representing the pores, has the following material moduli: $\mathbf{c}^{(2)}\approx 0$, $\mathbf{e}^{(2)}=0$, $\kappa_{jj}^{(2)}=\kappa_a$; where $\kappa_a$ is dielectric permittivity of vacuum $\kappa_a=\varepsilon_0=8.85\cdot10^{-12}$ (F/m) or air.

## 3. Algorithm of the representative volume generation for composites of 3-3 connectivity

We develop an algorithm for generating two-phase composite with 3-3 connectivity that consists of two stages. At the first stage, a minimal structure that ensures connectivity between two phases is constructed. At the second stage, auxiliary elements are added to the structure in order to achieve the required percentage of materials.

A representative volume has the shape of a cube and consists of $n^3$ cubic domains of equal size, which uniformly divide the sides of the volume. These cubic domains are generated according to the suggested algorithm to represent a composite structure. Each domain contains $8^3$ = 512 identical cubic elements, dividing each side of the cube in 8 segments. Number 8 for the domain division is chosen for the convenience of implementing numerical procedures that verify the phase connectivity and form data structures. Thus, a representative volume cube can consist of $(8n)^3$ cubes of smaller size, which are further considered as finite elements, constituting the mesh of the representative volume.

For all elements of the cubic domain, the algorithm generates label 1 or 2, defining the material number of the considered two-phase composite. Before the algorithm starts, all elements of the domain have label 2 of material 2. Then several elements of the domain change their labels from 2 to 1 in order to generate some initial distribution of material 1.

The procedure to obtain this initial distribution of elements with label 1 is as follows. At first, eight corner elements of the cubic domain and a randomly chosen support element receive label 1. The support element can be any element inside the domain, except for the corner elements and the anchor elements, located approximately in the middle of each domain edge, which ensure the connectivity of material 2 (see Fig. 1). Here elements with label 2 are marked in dark grey, elements with label 1 (the corner elements and the reference element) are marked in light grey, and the anchor elements are marked in grey.

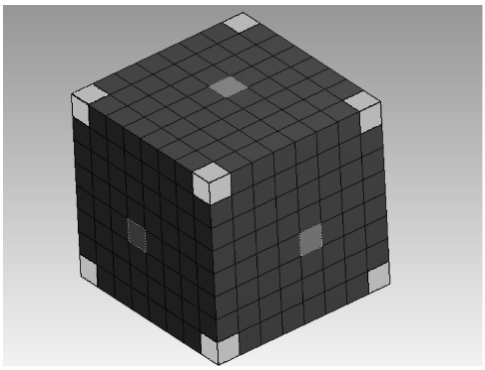

**Fig. 1.** Corner elements (light grey) and anchor elements (grey) in cubic domain.

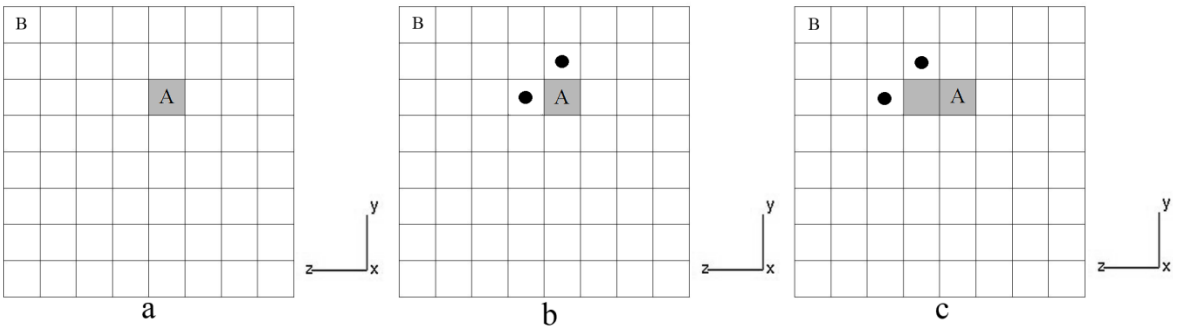


**Fig. 2.** Steps to build the shortest path from element A to element B.

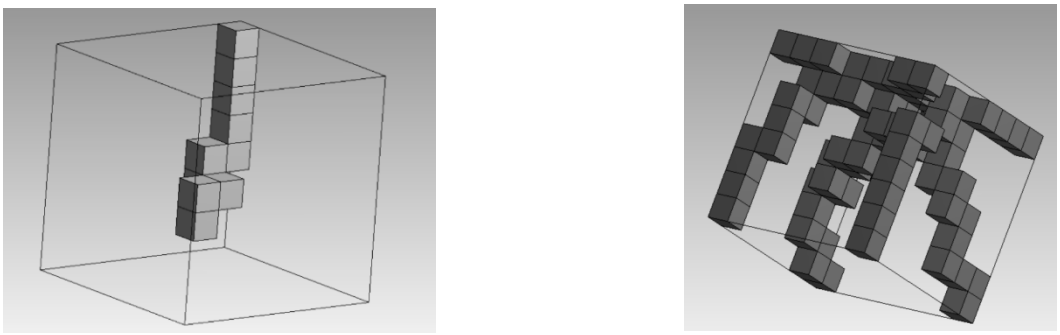

(a) (b)

**Fig. 3.** (a) Path from a support element to one corner element; (b) example of initial distribution of material 1.

Then the algorithm generates the paths from the support element to each of the corner elements. The procedure of generating a sequence of elements (path) from a support element (element A) to a certain corner element (element B) is illustrated by Fig. 2. Fig. 2a shows the

start and end elements of the path. The start element (element A) is marked by light grey. While constructing the sequence of elements from A to B, at each step the algorithm selects candidate elements (marked by dark circle) for the sequence. These candidate elements should satisfy the requirement to obtain the shortest path (see Fig. 2b) from start element A to end corner element B. The next element for the sequence is randomly chosen from the candidate elements and gets label 1 (marked by light grey in Fig. 2c). Then new candidate elements are selected in the same way. This process continues, until the sequence of elements reaches corner element B (Fig. 3a). The procedure of building the shortest path has the following limitation: the anchor elements at the domain edges, which ensure connectivity of material 2 (marked by grey in Fig. 1), cannot be the candidate elements for the shortest path. After building eight paths from the reference element to the corner elements, we get initial distribution of material 1 in the domain (see Fig. 3b).

At the end of the first stage of the algorithm, the connectivity of material 2 may be broken inside the domain. After conducting around 500 thousand numerical experiments, we have concluded that statistically this occurs in approximately 9% of the cases. Therefore, after finishing the first stage and obtaining the initial distribution of material 1, we check the connectivity of material 2. If the connectivity requirement is not satisfied, the constructed element sequence of material 1 is discarded and the algorithm starts again with new support element. The result of the first stage is the distribution of material 1, which in general occupies around 15% of the domain volume (from 73 to 82 elements).

At the second stage of the algorithm, the initial distribution of material 1 (marked by light grey in Fig. 4) is extended by other elements to achieve the required percentage of material 1. The algorithm randomly selects one of the elements from the element sequence with labels of material 2. Then all neighboring elements with label 2 become the candidate elements for extending the set. Among these candidate elements, the algorithm randomly selects one element, the addition of which will not violate the connectivity of material 2 (see Fig. 4). In Fig. 4, dark grey color indicates the anchor elements and cross indicates the elements of material 2, which cannot be removed from material 2 and added to material 1. Removal these elements will violate the connectivity of material 2. At this stage, the connectivity check is performed by using the algorithm of the breadth-first search on a graph, consisting of the elements of material 2 [5].

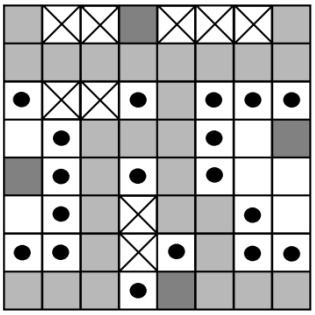

**Fig. 4.** Extension of the initial distribution of material 1.

The extension of the initial distribution continues until either the required percentage of material 1 is reached or the set of possible candidate elements becomes empty. We note that the composite structure is generated independently in every domain of the representative volume, because the support elements in each domain are randomly chosen. The global connectivity of both materials 1 and 2 is preserved due to the use of neighboring corner and anchor elements for neighboring domains.

In a series of numerical experiments, we have determined the ranges of the percentage content of materials in the final composite. Thus, Table 1 illustrates the correspondence between the required percentage content of material 1, denoted by *W*, and the resulting percentage content, denoted by *R*, which was obtained in the generated mesh. The difference between the required and the obtained percentages does not exceed 0.2 %.

Table 1. Results of 3-3 composite generation with various percentage content of material 1.

| | | | | | | | | |
|---|---|---|---|---|---|---|---|---|
| *W*, % | 15.00 | 20.00 | 25.00 | 30.00 | 35.00 | 40.00 | 45.00 | 50.00 |
| *R*, % | 15.43 | 20.12 | 25.00 | 30.08 | 35.16 | 40.04 | 45.12 | 50.00 |
| *W*, % | 55.00 | 60.00 | 65.00 | 70.00 | 75.00 | 80.00 | 85.00 | 90.00 |
| *R*, % | 55.08 | 60.16 | 65.04 | 70.12 | 75.00 | 80.08 | 85.16 | 90.04 |

Thus, the percentage of material 1 may vary from 15% to 95%. However, by changing the labels of the materials we can get the composite with the percentage of the required material ranging from 5% to 95%. Hence, the described algorithm enables us to generate 3-3 connectivity of composite structures with different percentages of the constituting phases, including the composites with very small or very large inclusions for one of the phases.

## 4. Results of numerical experiments

We note that the model of 3-0 connectivity in ACELAN-COMPOS allows phase inverting for a two-phase composite. For a porous composite, we can adopt that phase 1 is a piezoceramic material and phase 2 indicates pores. This case will be further referred to as case A. However, we can invert the phases and consider that phase 2 is a piezoceramic and phase 1 is a porous phase. Such case will be further referred to as case B. As it can be noted, the algorithm, described in Section 3, forms the phases, which are nonsymmetric with respect to the domain center. For phase 1, the connectivity at the transition from one domain to another is provided by the vertices of the domains. At the same time, the connectivity for phase 2 is ensured by the anchor elements, which are located close to the centers of the domain edges. Therefore, the distribution of phase 1 is more symmetric compared to the distribution of phase 2. Hence, we can conclude that case A, where phase 1 is a piezoceramic, is more preferable for simulating porous piezoceramic composites than case B.

Here we will compare results of the effective moduli calculation by using the algorithm, described in Section 3 and obtained from the solutions of problems (1) – (3) with five different types of boundary conditions (4) – (8) with similar results, obtained in ANSYS finite element package for the model that supports only the connectivity of a piezoceramic skeleton. A detailed description of this model can be found in [6]. Such model will be further referred to as 3-0(3) connectivity model, or case C.

Numerical experiments presented below were performed for a porous piezoceramic PZT-4. Table 2 contains the results of the effective moduli calculation for the fixed percentage content of material 2 (40%) and different numbers of finite elements in the representative volume of the composite. Here $n = 8$ indicates the case of one domain in the representative volume; $n = 16$ indicates two domains at the edges of the representative volume, and $n = 32$ stands for three domains at the representative volume edges, where $n$ is the number of finite elements along each representative volume edge. Letters a, b and c denote three different launches of the program for the representative volume generation. Table 3 contains similar results for 70% of material 2. The results, presented in Tables 2 and 3, were obtained for basic case A.

As the developed algorithm for 3-3 composite generation is to a great extent stochastic, the results, obtained for different launches of the program with the same input data, will be different. This difference can be observed from comparison of the corresponding columns *n*a,

*n*b and *n*c in Tables 2 and 3. This difference is small for small porosity (Table 2) and becomes larger for larger values of porosity (Table 3), especially for a small number of elements at the representative volume edge ($n = 8$).

Table 2. Effective moduli for piezoceramic PZT-4 with 40 % porosity for case A.

| Launch of the program | 8a | 8b | 8c | 16a | 16b | 16c | 32a | 32b | 32c |
|---|---|---|---|---|---|---|---|---|---|
| Porosity (%) | 40 | 40 | 40 | 40 | 40 | 40 | 40 | 40 | 40 |
| $c_{11}^{\text{eff}}, 10^{10}$ N/m$^2$ | 5.41 | 5.38 | 5.32 | 4.63 | 4.43 | 4.82 | 4.17 | 4.16 | 4.09 |
| $c_{12}^{\text{eff}}, 10^{10}$ N/m$^2$ | 2.41 | 2.33 | 2.17 | 1.94 | 1.87 | 1.93 | 1.68 | 1.71 | 1.67 |
| $c_{13}^{\text{eff}}, 10^{10}$ N/m$^2$ | 2.21 | 2.32 | 2.25 | 1.78 | 1.69 | 1.76 | 1.53 | 1.49 | 1.50 |
| $c_{33}^{\text{eff}}, 10^{10}$ N/m$^2$ | 4.37 | 4.55 | 4.49 | 3.73 | 3.55 | 3.52 | 3.32 | 2.27 | 3.29 |
| $c_{44}^{\text{eff}}, 10^{10}$ N/m$^2$ | 1.23 | 1.30 | 1.29 | 1.15 | 1.10 | 1.13 | 1.03 | 1.02 | 1.03 |
| $e_{31}^{\text{eff}}$, C/m$^2$ | –1.60 | –1.62 | –1.62 | –1.01 | –0.91 | –1.01 | –0.69 | –0.70 | –0.68 |
| $e_{33}^{\text{eff}}$, C/m$^2$ | 8.05 | 8.39 | 8.40 | 7.51 | 7.20 | 7.12 | 7.01 | 6.92 | 6.92 |
| $e_{15}^{\text{eff}}$, C/m$^2$ | 5.71 | 6.12 | 6.07 | 5.17 | 4.95 | 5.15 | 4.63 | 4.55 | 4.60 |
| $\kappa_{11}^{\text{eff}} / \varepsilon_0$ | 418 | 409 | 411 | 416 | 406 | 429 | 412 | 416 | 409 |
| $\kappa_{33}^{\text{eff}} / \varepsilon_0$ | 350 | 362 | 367 | 350 | 345 | 342 | 342 | 341 | 341 |

Table 3. Effective moduli for piezoceramic PZT-4 with 70 % porosity for case A.

| Launch of the program | 8a | 8b | 8c | 16a | 16b | 16c | 32a | 32b | 32c |
|---|---|---|---|---|---|---|---|---|---|
| Porosity (%) | 70 | 70 | 70 | 70 | 70 | 70 | 70 | 70 | 70 |
| $c_{11}^{\text{eff}}, 10^{10}$ N/m$^2$ | 1.73 | 2.26 | 1.89 | 1.24 | 1.40 | 1.23 | 0.97 | 0.98 | 0.98 |
| $c_{12}^{\text{eff}}, 10^{10}$ N/m$^2$ | 0.65 | 0.97 | 0.70 | 0.36 | 0.45 | 0.38 | 0.30 | 0.30 | 0.30 |
| $c_{13}^{\text{eff}}, 10^{10}$ N/m$^2$ | 0.54 | 0.64 | 0.57 | 0.35 | 0.38 | 0.36 | 0.27 | 0.25 | 0.27 |
| $c_{33}^{\text{eff}}, 10^{10}$ N/m$^2$ | 1.26 | 1.31 | 1.31 | 0.97 | 0.97 | 1.03 | 0.80 | 0.73 | 0.78 |
| $c_{44}^{\text{eff}}, 10^{10}$ N/m$^2$ | 0.44 | 0.49 | 0.47 | 0.33 | 0.33 | 0.34 | 0.26 | 0.24 | 0.26 |
| $e_{31}^{\text{eff}}$, C/m$^2$ | –0.37 | –0.54 | –0.39 | –0.13 | –0.15 | –0.09 | 0.05 | 0.05 | 0.06 |
| $e_{33}^{\text{eff}}$, C/m$^2$ | 2.83 | 2.82 | 2.85 | 2.37 | 2.34 | 2.52 | 2.04 | 1.89 | 2.00 |
| $e_{15}^{\text{eff}}$, C/m$^2$ | 1.92 | 2.26 | 2.06 | 1.43 | 1.42 | 1.46 | 1.06 | 1.00 | 1.07 |
| $\kappa_{11}^{\text{eff}} / \varepsilon_0$ | 184 | 215 | 191 | 172 | 188 | 174 | 169 | 175 | 173 |
| $\kappa_{33}^{\text{eff}} / \varepsilon_0$ | 153 | 139 | 142 | 144 | 133 | 143 | 136 | 132 | 135 |

The comparison of Tables 2 and 3 allows us to conclude that the number of elements in the representative volume significantly affects the values of the effective moduli, especially for highly porous composites. Large scatter in the values in Table 3 at $n = 8$, $n = 16$ and $n = 32$ can be explained by two facts. First, the characteristic features of the composite structure are not represented sufficiently for small $n$ ($n = 8$). Second, the effective moduli are determined by (4) – (8) as integral values by the representative volume from the stress and electric induction fields. Therefore, when the number $n$ of elements along the edges of the representative volume increases, the relative size of these elements decreases. Hence, for large

values of *n*, when the relative transverse dimension of a chain of finite elements in the piezoceramic becomes smaller, the chain becomes less stiff. This results in a decrease of the effective stiffness moduli and piezomoduli. Meanwhile, the values of the dielectric permittivities are less affected by the number of elements along the representative volume edge. Therefore, we can conclude that the choice of the representative volume for highly porous composites should be based not only on the convergence of results with increasing *n*, but also on the estimation of the ratio of characteristic lengths of the piezoceramic element chains to the transverse dimensions of these chains.

Tables 4 – 6 presents dependencies of the effective properties of the composite on the percentage content of the pores in the representative volume at the fixed number of finite elements along the representative volume edge ($n = 32$). These tables contain the results for all three cases, namely, for basic case A, for case B, where the composite phases are interchanged, and for case C, where the 3-0(3) algorithm is used with $n = 20$ [6].

Table 4. Effective stiffness moduli of piezoceramic for various porosity values.

| Modulus | Porosity / Case | 0 | 20 | 30 | 40 | 50 | 60 | 70 | 80 |
|---|---|---|---|---|---|---|---|---|---|
| $c_{11}^{\text{eff}}, 10^{10}$ N/m$^2$ | A | 13.9 | 8.48 | 5.99 | 4.17 | 2.69 | 1.72 | 0.97 | 0.49 |
| | B | 13.9 | 8.10 | 5.72 | 3.73 | 2.46 | 1.30 | 0.72 | 0.28 |
| | C | 13.9 | 9.23 | 6.85 | 5.05 | 3.31 | 2.08 | 1.27 | 0.68 |
| $c_{12}^{\text{eff}}, 10^{10}$ N/m$^2$ | A | 7.78 | 4.14 | 2.66 | 1.68 | 1.00 | 0.57 | 0.30 | 0.14 |
| | B | 7.78 | 3.85 | 2.44 | 1.43 | 0.86 | 0.42 | 0.20 | 0.06 |
| | C | 7.78 | 4.66 | 3.14 | 2.09 | 1.17 | 0.63 | 0.27 | 0.13 |
| $c_{13}^{\text{eff}}, 10^{10}$ N/m$^2$ | A | 7.43 | 3.85 | 2.44 | 1.53 | 0.88 | 0.51 | 0.26 | 0.11 |
| | B | 7.43 | 3.56 | 2.23 | 1.28 | 0.80 | 0.37 | 0.18 | 0.06 |
| | C | 7.43 | 4.28 | 2.84 | 1.85 | 1.06 | 0.52 | 0.24 | 0.10 |
| $c_{33}^{\text{eff}}, 10^{10}$ N/m$^2$ | A | 11.5 | 6.87 | 4.85 | 3.32 | 2.12 | 1.33 | 0.80 | 0.39 |
| | B | 11.5 | 6.52 | 4.52 | 2.97 | 1.95 | 1.06 | 0.58 | 0.25 |
| | C | 11.5 | 7.29 | 5.38 | 3.90 | 2.73 | 1.63 | 0.91 | 0.47 |
| $c_{44}^{\text{eff}}, 10^{10}$ N/m$^2$ | A | 2.56 | 1.79 | 1.39 | 1.03 | 0.71 | 0.46 | 0.26 | 0.11 |
| | B | 2.56 | 1.74 | 1.34 | 0.96 | 0.68 | 0.39 | 0.20 | 0.08 |
| | C | 2.56 | 1.84 | 1.45 | 1.09 | 0.73 | 0.44 | 0.23 | 0.10 |

Table 5. Effective piezomoduli of piezoceramic for various porosity values.

| Modulus | Porosity / Case | 0 | 20 | 30 | 40 | 50 | 60 | 70 | 80 |
|---|---|---|---|---|---|---|---|---|---|
| $e_{31}^{\text{eff}}$, C/m$^2$ | A | –5.2 | –2.59 | –1.42 | –0.69 | –0.22 | 0.00 | 0.05 | 0.01 |
| | B | –5.2 | –2.40 | –1.33 | –0.58 | –0.20 | 0.04 | 0.03 | 0.01 |
| | C | –5.2 | –3.14 | –2.09 | –1.32 | –0.74 | –0.43 | –0.21 | –0.10 |
| $e_{33}^{\text{eff}}$, C/m$^2$ | A | 15.1 | 11.47 | 9.24 | 7.01 | 4.87 | 3.25 | 2.04 | 1.02 |
| | B | 15.1 | 11.25 | 8.89 | 6.53 | 4.62 | 2.71 | 1.54 | 0.68 |
| | C | 15.1 | 11.45 | 9.58 | 7.71 | 5.97 | 3.89 | 2.32 | 1.24 |
| $e_{15}^{\text{eff}}$, C/m$^2$ | A | 12.7 | 8.51 | 6.44 | 4.63 | 3.07 | 1.93 | 1.06 | 0.46 |
| | B | 12.7 | 8.24 | 6.15 | 4.24 | 2.90 | 1.60 | 0.83 | 0.31 |
| | C | 12.7 | 8.89 | 6.86 | 5.04 | 3.30 | 1.96 | 0.99 | 0.44 |

Table 6. Effective dielectric permittivites of piezoceramic for various porosity values.

| Modulus | Porosity / Case | 0 | 20 | 30 | 40 | 50 | 60 | 70 | 80 |
|---|---|---|---|---|---|---|---|---|---|
| $\kappa_{11}^{\text{eff}} / \varepsilon_0$ | A | 730 | 581 | 497 | 412 | 326 | 247 | 169 | 109 |
| | B | 730 | 578 | 494 | 405 | 316 | 221 | 153 | 81 |
| | C | 730 | 588 | 511 | 438 | 350 | 265 | 191 | 121 |
| $\kappa_{33}^{\text{eff}} / \varepsilon_0$ | A | 635 | 492 | 418 | 342 | 265 | 197 | 136 | 84 |
| | B | 635 | 487 | 412 | 332 | 262 | 184 | 124 | 68 |
| | C | 635 | 488 | 415 | 343 | 271 | 198 | 130 | 75 |

Tables 4 – 6 illustrate known dependencies of the effective moduli, decreasing at the porosity growth ([2, 4, 6] and others). We can also note that the model of 3-0(3) connectivity (case C) is the most stiff, the model of 3-3 connectivity with inverted phases (case B) has the lowest stiffness, and the basic model of 3-3 connectivity (case A) lies in the middle between these two cases with respect to stiffness.

## 5. Conclusions

The paper has described the methods of homogenization for porous piezoceramic composite and the algorithm for a representative volume generation for 3-3 connectivity composite implemented in ACELAN-COMPOS finite element software package, developed by the authors. The suggested algorithm allows setting the percentage content of the composite phases and the number of elements along the representative volume edge. The numerical experiments performed have shown a wide range of the algorithm applicability (5 – 95%). The effective material properties of porous piezoceramic were calculated for different porosity values and different number of elements in the representative volume. The numerical results obtained have demonstrated that the values of the effective moduli are significantly influenced by the representative volume sizes and the structure of the composite phases in case of highly porous piezoceramic.

***Acknowledgements.*** *The work was supported by the Ministry of Education and Science of Russian Federation, competitive part of state assignment, No. 9.1001.2017/PCh.*

## References

[1] E. Ringgaard, F. Lautzenhiser, L.M. Bierregaard, T. Zawada, E. Molz // *Materials* **8(12)** (2015) 8877.

[2] A.N. Rybyanets // *IEEE Trans. Ultrason. Ferroelectr. Freq. Control* **58** (2011) 1492.

[3] N.V. Kurbatova, D.K. Nadolin, A.V. Nasedkin, A.A. Nasedkina, P.A. Oganesyan, A.S. Skaliukh, A.N. Soloviev, In: *Advanced Structured Materials* **59** (Springer, Singapore, 2017), p. 133.

[4] A.V. Nasedkin, M.S. Shevtsova, In: *Ferroelectrics and Superconductors: Properties and Applications*, ed. by I.A. Parinov (Nova Science Publishers, NY, 2011), p. 231.

[5] T.H. Cormen, C.E. Leiserson, R.L. Rivest, C. Stein, In: *Introduction to Algorithms* (MIT Press and McGraw-Hill, 2001), p. 531.

[6] A.V. Nasedkin, In: *Advanced Materials – Studies and Applications*, ed. by I.A. Parinov, S.H. Chang, S. Theerakulpisut (Nova Science Publishers, NY, 2016), p. 109.